International Journal of Optics and Applications 2017, 7(4): 69-74
DOI: 10.5923/j.optics.20170704.01

Phase Gradient Retrieval from Fringes Pattern by Using of Two-dimensional Continuous Wavelet Transforms

A. Ghlaifan, Y. Tounsi, D. Muhire, A. Nassim*

Measurement and Control Instrumentation Laboratory IMC, Physics Department, Chouaib Doukkali University, El Jadida, Morocco

Abstract The central goal of this paper is to present an algorithm for optical phase gradient evaluation from only one fringe pattern using the two-dimensional continuous wavelet transform (2D_CWT) analysis. The phase gradient is computed from the extremum scales correspond to the maximum ridge of the wavelet coefficients modulus. Spatial modulation process is realized by combining two shifted fringes patterns, we use only single fringe pattern and we suggest to generate its quadrature using spiral phase transform SPT. The obtained results with computer simulation and image quality index values show a good performance of the proposed algorithm, and eventually, we can reconstruct the spatial phase distribution by integrating numerically the phase gradient along x and y-direction. Also, experimental results are given by exploiting speckle fringe correlation recorded in digital speckle pattern interferometry.

Keywords Continuous wavelet transforms CWT, Wavelet ridge, Phase gradient extraction

1. Introduction

Optical phase extraction becomes a key technique in the analysis of the fringe pattern given in interferometric metrology. The phase distribution encoded in the recorded fringe pattern intensity provides full-field measurements of physical magnitude like displacement, strain, temperature, refractive index changes. The phase shifting [1] and the Fourier transform methods [2] are the most common techniques used to extract phase from the fringe pattern. Several authors have reported the use of the wavelet transform to retrieve phase distributions encoded by fringes pattern [3, 4].

Two-dimensional continuous wavelet transform (2D-CWT) techniques are used to successfully demodulate fringe patterns [5, 6]. These algorithms give a wrapped phase distribution from modulated fringe patterns due to use of arctangent [7], thus, phase unwrapping is necessary, and phase gradient leads directly to continuous phase distribution phase distribution [8, 9]. Avoiding the complex step of the phase unwrapping. We present here a study of the phase gradient extraction from a single fringe pattern using the two-dimensional continuous wavelet transform algorithm 2D-CWT; it is easy to compute the phase gradient from maximums scales relating to the ridge point of the wavelet coefficient modules, which are integrated to give directly the continuous phase distribution.

* Corresponding author:
nassim.a@ucd.ac.ma (A. Nassim)
Published online at http://journal.sapub.org/optics

The first section of this paper will examine the fringe pattern intensity distribution analysis using two-dimensional continuous wavelet transform (2D-CWT). The second part presents the algorithm for extraction of phase gradient from ridge wavelet and we are finishing the work by presenting differents obtained results using computer simulation and an experimental fringe pattern given from digital speckle pattern interferometry.

2. Fringe Pattern Analysis by 2D Continuous Wavelet Transform

An interference fringe pattern intensity distribution is commonly expressed as:

$$f = a(x, y) + b(x, y) \cdot \cos(\varphi(x, y)) \qquad (1)$$

Where $a(x, y)$ presents the background illumination, $b(x, y)$ denotes modulation factor of the fringe pattern, and $\varphi(x, y)$ is the phase distribution related to the desired physical magnitude. Since fringe pattern can be presented in digital format, the image processing techniques can be exploited to analyze them. Between these techniques, 2-CWT (two-dimensional continuous wavelet transform) has been successfully applied since it is robust and particularly helpful for detecting the characteristics of local fringes [10, 11].

Compared with the one-dimensional CWT algorithm [12], the 2D-CWT algorithm is more suitable for interferogram analysis due to its multiscale zooming capabilities.

The wavelet coefficients can be calculated by the correlation product between an image and the mother wavelet with different values of dilatation and angle of orientation, and it is a measure of the local similarity between them, the wavelet coefficients of a given signal $f(x,y)$ can be defined as:

$$w(\mathrm{t},\mathrm{d},s,\theta)= s^{-2}\iint f(x,y)\cdot\psi^{*}(s^{-1}R_{-\theta}(x-t,y-d))dxdy \tag{2}$$

Where the symbol * denoted the complex conjugate operator, t and d are respectively the translation parameters on x and y directions, s is a scale vector, θ is a rotation angle, ψ is the 2D mother wavelet and R_θ is the conventional 2x2 rotation matrix corresponding to θ.

$$R_\theta=(\mathrm{x}\cdot\cos\theta+y\cdot\sin\theta,\mathrm{y}\cdot\cos\theta-\mathrm{x}\cdot\sin\theta) \tag{3}$$

For the purpose of rigorous derivation, the most widely used 2D complex Morlet wavelet is employed here. The 2D complex Morlet just can be used to demodulate the fringe pattern with 2D-CWT, it is essentially a plan wave within a Gaussian window is given by:

$$\psi_m=\exp(-(x^2+y^2)/2)\cdot\exp(ik_0(x\cdot\cos\theta+y\cdot\sin\theta) \tag{4}$$

Where k_0 is a fixed spatial frequency, and chosen to be about 5 to 6 to satisfy the admissibility condition [13], and $i^2=-1$ represents the complex unit.

In the 2D-CWT, for the fringe pattern, the wavelet rotates at the angle of θ, and scans the whole fringe pattern across the two direction x and y by translation t and d respectively, $s>0$ is the scale factor.

3. Phase Gradient Retrieval from Wavelet Ridge

The analysis in CWT wavelet domain needs a fringe pattern with the spatial carrier in a chosen direction, for this reason, and using an appropriate modulation rate m, we combine numerically fringe pattern and its quadrature with the matrix cos(mx) and sin(mx) respectively to derive the modulated fringe pattern with a digital spatial frequency carrier [14]. Removing the background illumination from the intensity distribution of fringe pattern expressed in equ (1), by a low pass filter, it becomes as:

$$\tilde{f}(x,y)=b(x,y)\cdot\cos(\varphi(x,y)) \tag{5}$$

Recently, Larkin and all have proposed spiral phase quadrature transform (SPT) for the two-dimensional fringe pattern [15, 16]. Spiral phase transform of f is defined as:

$$SPT(\tilde{f})=j\cdot\exp(j\cdot D)\cdot b\cdot\sin(\varphi) \tag{6}$$

The quadrature term (b.sinφ) appears in the equation, where j is a complex unit verifying $j^2=-1$ and D represents direction map. From the equation (6), we obtain sine fringe pattern (quadrature) as:

$$b\cdot\sin(\varphi)=-j\cdot\exp(-j\cdot D)\cdot SPT(\tilde{f}) \tag{7}$$

The direction map is giving in this paper as it is presented in [17], the ratio between the gradient of the phase in x and y is expressed as:

$$\tan(D)=\nabla_y\varphi/\nabla_x\varphi \tag{8}$$

The problem in this equation is that phase is unknown, so instead the direction map, we define orientation map formulated as:

$$\tan(\beta)=\nabla_y\tilde{f}/\nabla_x\tilde{f} \tag{9}$$

Then, orientation and direction map are related by:

$$\exp(\mathrm{j}\cdot D)=\pm\exp(\mathrm{j}\cdot\beta) \tag{10}$$

So, from this similarity between the two magnitudes, we define the quadrature map as:

$$q(x,y)=b\cdot\sin(\varphi)=-j\cdot\exp(-j\cdot\beta)\cdot SPT(\tilde{f}) \tag{11}$$

We obtain modulated fringe pattern digitally by introducing spatial carrier characterized by their modulation ratio m and the intensity distribution in a modulated fringe pattern defined as follow:

$$f_m=\tilde{f}\cdot\cos(\mathrm{m}\cdot\mathrm{x})-\mathrm{q}\cdot\sin(\mathrm{m}\cdot\mathrm{x}) \tag{12}$$

This gives

$$f_m=b\cdot\cos(\varphi+m\cdot x) \tag{13}$$

A phase-modulated carrier is then added to the phase of interest to enable the wavelet phase extraction.

Computing the 2D-CWT wavelet coefficients of the modulated fringe pattern, we extract the wavelet ridge defined as the maximum of the obtained coefficients and its modulus should have a maximum value when the dilatation and rotation of the mother wavelet and the fringe pattern are more locally similar.

A new matrix is constructed by picking up the maximum value of each column of the wavelet coefficient modulus array, this is called the wavelet ridge, and then, the corresponding scale value is determined from the ridge wavelet. By repeating this process to all pixel of the fringe pattern, the phase gradient is then estimated.

The local maxima of the modulus of wavelet coefficients at all positions make up of the wavelet ridge [18, 19], supposing that the scales relating to the ridge points, the maximum scales $s_{\max}$ correspond to the maximum ridge of the wavelet coefficients modulus is defined as:

$$(s_{\max},\theta)=\underset{s\in R^{+},\theta\in[0,2\pi]}{\arg\max}\left|w(t,d,s,\theta)\right| \tag{14}$$

Where $s_{\max}$ represent the scale value for maxima.

In term of representation of cwt transform, given a 2D signal, we produce a 4D representation which cannot be readily plotted or visualized. There exist several possible representations [20]. That the CWT can determine the local frequency [21], we have a natural way to detect the phase gradient that can be obtained from the local frequencies as:

$$\nabla\varphi = \left(k_0 + (k_0{}^2 + 2)^{\frac{1}{2}} / 2s_{\max}\right) - m \qquad (15)$$

Where m is the modulation ratio.

4. Computer Simulation and Application on Real Fringes

To prove the effectiveness of the proposed method, we have tested it with simulated fringe patterns using MatLab software; the test phase distribution shown in figure (1.a) that we used has the following expression:

$$\varphi(x,y) = 0.15\cdot((x-128)^2 + (x-128)^2)^{1/2} \qquad (16)$$

Where x and y are the pixel coordinates. The horizontal and vertical phase gradient respectively simulated from the phase is shown in the figure. (1.b) and (1.c), figure (1.d) shows the three-dimensional representation of phase distribution and its one dimensional plotted line profile along row 128 is showed in figure (1.e).

In figure (2.b) we present the fringe pattern coded by the known simulated phase, and its quadrature obtained by spiral phase transforms SPT presented in figure (2.b). By combining numerically the fringe pattern and its quadrature, we obtained the modulated fringe pattern shown in figure (2.c) with a spatial carrier of frequency m = 1.5 red/pixel.

The 2D-CWT is applied to demodulate the modulated fringe pattern with both horizontal orientation $\theta = 0^\circ$, vertical orientation $\theta = 90^\circ$, and a scale vector vary from 2 to 12 with increments of 0.01, we obtain the results presented in figure (3). The right column present the 3d plotted original phase gradient distribution along x and y-direction. The middle column presents the retrieved phase gradient by using the proposed algorithm, and the left column presents the plotted profile along one row from original and estimated phase gradient.

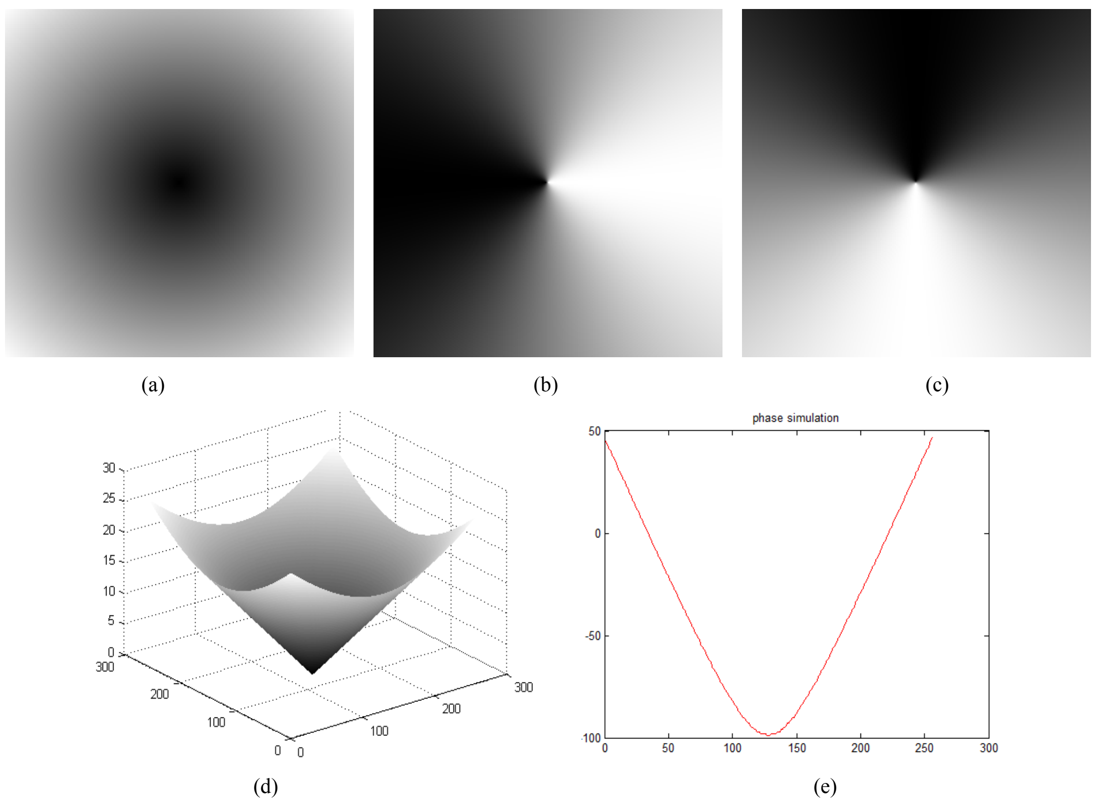

Figure 1. Computer simulation (a) simulated phase map (b, c) simulated horizontal and vertical Phase gradient (d) 3d plotted phase map and (e) plotted line profile for row (:,128)

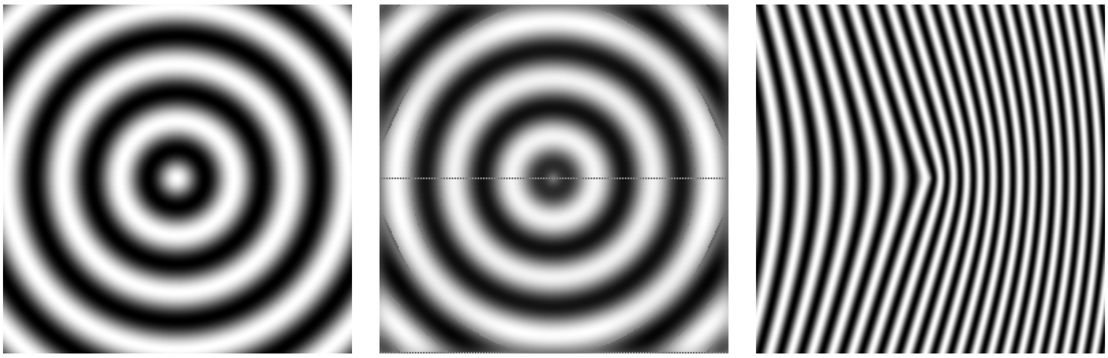

(a) (b) (c)

Figure 2. Results of computer simulation (a) fringe pattern intensity distribution (b) quadrature map obtained by SPT (c) fringe pattern with spatial carrier

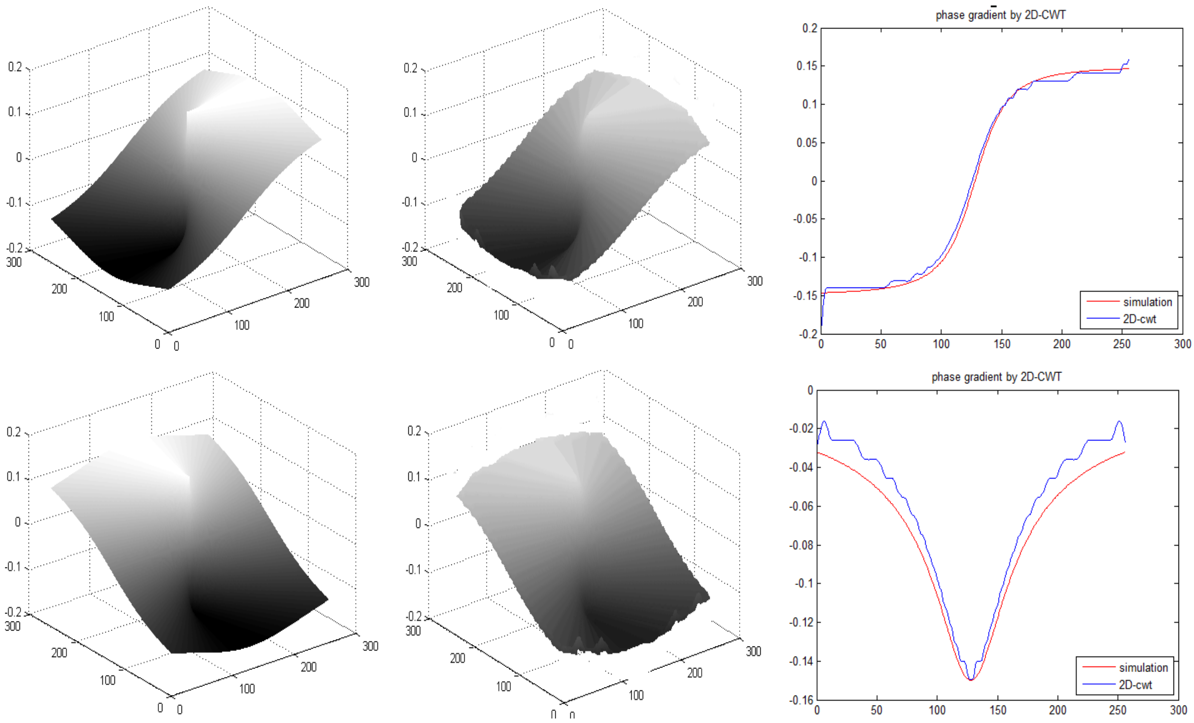

Figure 3. **Right**: Original phase gradient distribution along x and y-direction. **Middle**: Retrieved phase gradient. **Left**: Plotted profile along one row from original and estimated phase gradient

By implementing a numerical integration of the two phase gradient, we obtain directly the continuous phase distribution without phase unwrapping step as illustrated in figure 4.

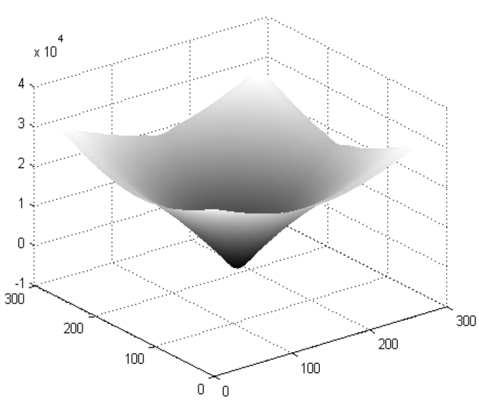

Figure 4. Profile of the obtained phase distribution by numerical integration

The performance of evaluation algorithm is measured by image quality assessment (Q) [22]. This quality index model any distortion as a combination of three different factors: loss of correlation, luminance distortion, and contrast distortion. The first component is the correlation coefficient between the original and the test images x and y, which measures the degree of linear correlation between them. It is defined as:

$$Q_1 = \sigma_{xy} / \sigma_x \sigma_y \tag{17}$$

The second component measures the mean luminance between x and y, which is defined as:

$$Q_2 = 2\overline{x}.\overline{y} / \left((\overline{x})^2 + (\overline{y})^2 \right) \tag{18}$$

The third component measures the similarity the contrasts of the image are defined as follows:

$$Q_3 = 2\sigma_x\sigma_y / \left(\sigma_x^2 + \sigma_y^2\right) \quad (19)$$

The proposed image quality index is defined as a product of three components:

$$Q = Q_1 \times Q_2 \times Q_3 \quad (20)$$

Where $\bar{x}$ and $\bar{y}$ presents the average of the image x and y, σ_x and σ_y the standard deviation of the two images, respectively. The Q values are in the range [-1, 1] where 1 is satisfied for an exact retrieval characteristic. The table below shows the metric value given by Q index that compares the original phase gradient distribution with there obtained by 2D-CWT.

Table 1. Quality measurement by metric similarity Q

Retrieved characteristic map	Q index value
Horizontal phase gradient	0.90
Vertical phase gradient	0.90
Recovered phase distribution with numerical integration	0.96

After validation of the proposed cwt algorithm by simulation and her good accuracy showed using Q index, we exploit an experimental fringe recorded using digital speckle pattern interferometry [23].

The experimental evaluation of the proposed method is performed with a speckle fringe correlation obtained in speckle interferometry, it is a powerful optical measurement technique used for industrial measurements to study deformations, vibrations, defects, and damages assessments [23]. experimentally, speckle pattern exposure of the object is taken in one position. Then the object is deformed, and another exposure is taken. We exploit in this part the speckle fringe correlation of fiber carbon given by *4d technology society®*. Figure (5a) and figure (5b) present the recorded speckle patterns after and before deformation, these two speckle patterns are subtracted, and their difference is squared in order to obtain speckle correlation fringes corresponding to the object's deformation as shown by a figure (5c).

Fringes correlation are characterized by a strong speckle noise defined as a granular structure resulting from self-interference of coherent waves randomly scattered from a rough surface, making it capable of giving the measurement of displacements with an accuracy of the order of wavelength used. The proposed technique is very sensitive to speckle noise, for this reason, speckle fringes correlation undergo to a denoising step to reduce this noise. After denoising step, we apply the proposed technique; we give the horizontal and vertical phase gradient illustrated respectively in figure (6a) and figure (6b). A two-dimensional numerical integration of the two phase gradient in the two directions provides the continuous optical phase distribution presented in figure (6c).

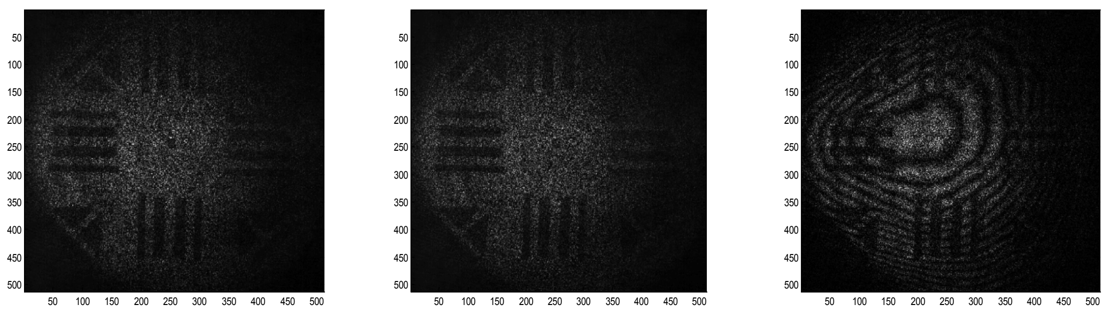

(a) (b) (c)

Figure 5. The recorded speckle pattern. (a) After deformation, (b) before deformation, (c) speckle fringe correlation

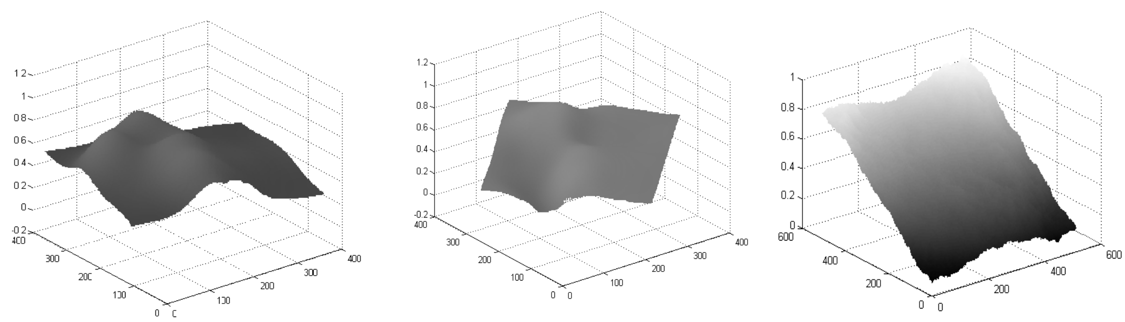

(a) (b) (c)

Figure 6. The estimated features after filtering step, (a) horizontal phase derivative, (b) vertical phase derivative, (c) phase distribution obtained by numerical integration

5. Conclusions

The aim of this paper was to extract phase gradient distribution from a single fringe pattern with a spatial carrier using the 2-CWT algorithm. This study has shown that we can use only a single fringe pattern and generate its quadrature by spiral phase transform SPT, and this makes us to introduced digitally the spatial carrier. The performance of the proposed algorithm has been evaluated with the good accuracy by using generated fringes pattern by computer simulation. In an experimental context, we have applied the 2-CWT algorithm to a speckle fringe correlation after a speckle noise removing step.

ACKNOWLEDGMENTS

The authors want to thank Dr. Neal Brock and Dr. J. C. Wyant from 4D Technology for providing them the experimentally shifted fringe patterns.

REFERENCES

[1] G. Lai et T. Yatagai, « Generalized phase-shifting interferometry », *J. Opt. Soc. Am. A, JOSAA*, vol. 8, n° 5, p. 822‑827, mai 1991.

[2] Q. Kemao, « Two-dimensional windowed Fourier transform for fringe pattern analysis: Principles, applications and implementations », *Optics and Lasers in Engineering*, vol. 45, n° 2, p. 304‑317, févr. 2007.

[3] S. Mallat, *A Wavelet Tour of Signal Processing*. Academic Press, 1999.

[4] M. Afifi, A. Fassi-Fihri, M. Marjane, K. Nassim, M. Sidki, et S. Rachafi, « Paul wavelet-based algorithm for optical phase distribution evaluation », *Optics Communications*, vol. 211, n° 1, p. 47‑51, oct. 2002.

[5] M. A. Gdeisat, D. R. Burton, et M. J. Lalor, « Spatial carrier fringe pattern demodulation by use of a two-dimensional continuous wavelet transform », *Appl Opt*, vol. 45, n° 34, p. 8722‑8732, déc. 2006.

[6] A. Z. Abid, M. A. Gdeisat, D. R. Burton, M. J. Lalor, et F. Lilley, « Spatial fringe pattern analysis using the two-dimensional continuous wavelet transform employing a cost function », *Appl Opt*, vol. 46, n° 24, p. 6120‑6126, août 2007.

[7] J. Zhong et J. Weng, « Spatial carrier-fringe pattern analysis by means of wavelet transform: wavelet transform profilometry », *Appl. Opt., AO*, vol. 43, n° 26, p. 4993‑4998, sept. 2004.

[8] A. Federico et G. H. Kaufmann, « Evaluation of the continuous wavelet transform method for the phase measurement of electronic speckle pattern interferometry fringes », *OE, OPEGAR*, vol. 41, n° 12, p. 3209‑3217, déc. 2002.

[9] L. R. Watkins, S. M. Tan, et T. H. Barnes, « Determination of interferometer phase distributions by use of wavelets », *Opt. Lett., OL*, vol. 24, n° 13, p. 905‑907, juill. 1999.

[10] L. R. Watkins, « Phase recovery from fringe patterns using the continuous wavelet transform », *Optics and Lasers in Engineering*, vol. 45, n° 2, p. 298‑303, févr. 2007.

[11] J. Zhong et J. Weng, « Phase retrieval of optical fringe patterns from the ridge of a wavelet transform », *Opt. Lett., OL*, vol. 30, n° 19, p. 2560‑2562, oct. 2005.

[12] P. Tomassini *et al.*, « Analyzing laser plasma interferograms with a continuous wavelet transform ridge extraction technique: the method », *Appl Opt*, vol. 40, n° 35, p. 6561‑6568, déc. 2001.

[13] C. Torrence et G. P. Compo, « A Practical Guide to Wavelet Analysis », *Bull. Amer. Meteor. Soc.*, vol. 79, n° 1, p. 61‑78, janv. 1998.

[14] E. M. Barj, M. Afifi, A. A. Idrissi, S. Rachafi, et K. Nassim, « A digital spatial carrier for wavelet phase extraction », *Optik - International Journal for Light and Electron Optics*, vol. 116, n° 11, p. 507‑510, oct. 2005.

[15] K. G. Larkin, D. J. Bone, et M. A. Oldfield, « Natural demodulation of two-dimensional fringe patterns. I. General background of the spiral phase quadrature transform », *J Opt Soc Am A Opt Image Sci Vis*, vol. 18, n° 8, p. 1862‑1870, août 2001.

[16] K. G. Larkin, « Natural demodulation of two-dimensional fringe patterns. II. Stationary phase analysis of the spiral phase quadrature transform », *J Opt Soc Am A Opt Image Sci Vis*, vol. 18, n° 8, p. 1871‑1881, août 2001.

[17] J. Vargas, R. Restrepo, J. C. Estrada, C. O. S. Sorzano, Y.-Z. Du, et J. M. Carazo, « Shack-Hartmann centroid detection using the spiral phase transform », *Appl Opt*, vol. 51, n° 30, p. 7362‑7367, oct. 2012.

[18] H. Liu, A. N. Cartwright, et C. Basaran, « Moiré interferogram phase extraction: a ridge detection algorithm for continuous wavelet transforms », *Appl. Opt., AO*, vol. 43, n° 4, p. 850‑857, févr. 2004.

[19] S. Li, X. Su, et W. Chen, « Wavelet ridge techniques in optical fringe pattern analysis », *J. Opt. Soc. Am. A, JOSAA*, vol. 27, n° 6, p. 1245‑1254, juin 2010.

[20] J.-P. Antoine, R. Murenzi, P. Vandergheynst, et S. T. Ali, *Two-Dimensional Wavelets and their Relatives*, 1 edition. Cambridge: Cambridge University Press, 2008.

[21] N. Delprat, B. Escudie, P. Guillemain, R. Kronland-Martinet, P. Tchamitchian, et B. Torresani, « Asymptotic wavelet and Gabor analysis: extraction of instantaneous frequencies », *IEEE Transactions on Information Theory*, vol. 38, n° 2, p. 644‑664, mars 1992.

[22] Z. Wang et A. C. Bovik, « A universal image quality index », *IEEE Signal Processing Letters*, vol. 9, n° 3, p. 81‑84, mars 2002.

[23] J. N. Butters et J. A. Leendertz, « Speckle pattern and holographic techniques in engineering metrology », *Optics & Laser Technology*, vol. 3, n° 1, p. 26‑30, févr. 1971.